Available online at www.sciencedirect.com
SCIENCE DIRECT
Thermochimica Acta 443 (2006) 109–115
thermochimica acta
www.elsevier.com/locate/tca

# Studies on lattice thermal expansion and XPS of $ThO_2$–$NdO_{1.5}$ solid solutions

G. Panneerselvam [a], M.P. Antony [a,*], T. Vasudevan [b]

[a] *Fuel Chemistry Division, Indira Gandhi Centre for Atomic Research, Kalpakkam 603 102, India*
[b] *Department of Industrial Chemistry, Alagappa University, Karaikkudi 630 003, India*

Received 15 December 2005; received in revised form 1 February 2006; accepted 6 February 2006
Available online 28 February 2006

**Abstract**

The lattice parameter changes with respect to temperature (*T*) have been measured by high temperature X-ray diffraction (HTXRD) technique for $ThO_2$–$NdO_{1.5}$ solid solutions containing 23.8 and 42.5 mol% $NdO_{1.5}$ in the temperature range from 298 to 2000 K. The temperature versus lattice parameter data have been made use of in calculating the lattice thermal expansivity. The values of thermal expansion of the solid solutions were found to be increased with increase in neodymium oxide content and temperature. The mean linear thermal expansion coefficients in this temperature range for $ThO_2$–$NdO_{1.5}$ solid solutions are $12.28 \times 10^{-6}$ and $12.90 \times 10^{-6}\,K^{-1}$, respectively. The binding energies of Th $4f_{7/2}$ and Nd $3d_{5/2}$ energy levels of the solid solutions containing 13.1, 23.8, 31.9, 37.2 and 42.5 mol% $NdO_{1.5}$ and two-phase mixtures containing 47.6 and 51.8 mol% $NdO_{1.5}$ were experimentally determined by X-ray photoelectron spectroscopy (XPS).


*Keywords:* Thoria; Neodymium oxide; Solid solution; Thermal expansion; XRD; XPS

## 1. Introduction

The Indian Nuclear program (INP) envisages the use of thoria-based fuel in the third phase of nuclear power generation [1]. The thoria-based fuel will consist of solid solution of thorium – uranium and thorium – plutonium in the form of their oxides. The former will contain 2.5 mol% $UO_2$ while the latter about 4 mol% $PuO_2$. During irradiation of the fuel in the nuclear reactor, two types of solid fission products are found viz. metallic and non-metallic inclusions [2–4]. Among the non-metallic solid fission product compounds, the rare-earth oxides, $Ln_2O_3$ (Ln = La, Ce, Y, Nd, Sm, Eu and Gd), $ZrO_2$ and alkaline earth oxides MO (M = Sr and Ba) are the major inclusions. These fission products are known to form solid solutions with $UO_2$, while mainly rare-earth oxides are known to be soluble in the $ThO_2$ and $(U,Th)O_2$ lattice [5–7]. Thorium and rare-earth (RE) oxides have pivotal importance in nuclear industry. The properties of these compounds and their interaction products at high temperature are of interest in the solid-state chemistry of oxide nuclear fuels. Among various rare earths, neodymium is one of the major fission products that is present in the oxide form, $Nd_2O_3$ [8]. $ThO_2$ can dissolve considerable amounts of rare-earth oxides in its fluorite ($CaF_2$) lattice [9–14]. The solubility of $NdO_{1.5}$ in $ThO_2$ at 1473 K have been measured and found to be in the range 45.7–46.2 mol% [15]. The changes in lattice parameter of thoria with possible fission product additions have already been reported in the literature [2,5,16]. However, not much data are available in open literature on the thermal expansion characteristics of $ThO_2$–$NdO_{1.5}$ solid solutions.

In this context, we have been investigating various thorium-based mixed oxide systems. One of the major activities is on the thermal expansion behaviour of different thoria-based systems having relevance to the proposed thorium oxide-based nuclear reactors. An attempt has been made to measure the lattice thermal expansion of $ThO_2$–$NdO_{1.5}$ solid solutions by high temperature X-ray powder diffraction technique.

In addition, the information on the binding energies of Th $4f_{7/2}$ and Nd $3d_{5/2}$ levels in $ThO_2$–$NdO_{1.5}$ solid solutions is also essential to understand the chemical state of the cations in the solid solutions. The relative metallic valency is expected to have an influence on various physicochemical properties of the solid solutions. To the best of our knowledge, no data on the

* Corresponding author. Tel.: +91 44 27480098; fax: +91 44 27480065.
*E-mail addresses:* mpa@igcar.gov.in, mpa@igcar.ernet.in (M.P. Antony).

0040-6031/$ – see front matter © 2006 Elsevier B.V. All rights reserved.
doi:10.1016/j.tca.2006.02.009

binding energies of cations in these solid solutions are available in the open literature. Hence, the binding energies of Th $4f_{7/2}$ and Nd $3d_{5/2}$ photoelectron spectra for $ThO_2$–$NdO_{1.5}$ solid solutions have been experimentally studied by X-ray photoelectron spectroscopy. The results of the investigations are reported in this paper.

## 2. Experimental details

### 2.1. Sample preparation

Thorium nitrate [$Th(NO_3)_4$ $4H_2O$] and neodymium oxide $Nd_2O_3$ (99.97% pure) used in the present work were procured from M/s. Indian Rare Earths Ltd. Carefully weighed quantities of thorium nitrate and calcined neodymium oxide were dissolved in water and concentrated nitric acid, respectively. Subsequently, their hydroxides were co-precipitated by the addition of aqueous ammonia under continuous stirring. The precipitate was dried in air at 323 K in an oven, followed by calcination at 873 K for about 4 h. The calcined powder was cold compacted at 500 MPa, into pellets of about 10 mm diameter and 2–3 mm thickness, by using a hydraulic press. The cold compaction was made without the addition of any binder or lubricant. The green compacts thus prepared were sintered in air at different temperature in the range 900–1473 K for about 6 h. It is found that sintering at 1473 K for about 6 h resulted in fairly dense ceramic compacts. These solid solutions were characterized by standard wet-chemical analysis. For the compositional characterization of $ThO_2$–$NdO_{1.5}$ solid solutions, a known amount (0.5–1 g) of the sample was dissolved in hot concentrated nitric acid, in presence of traces of HF. The analysis for thorium was carried out by titration with DTPA (diethylene triaminepentaacetic acid) under controlled pH condition [17,18]. The strongly acidic solution containing the sample was first diluted; the pH was then brought down to about 2.5 by adding dilute aqueous ammonia. Xylenol orange was used as the indicator. For the determination of neodymium content, a known excess of DTPA was added; the pH was adjusted to be in the range to 5–5.5 by adding solid urotropine. The excess of DTPA was titrated with 0.05 M lead nitrate solution with xylenol orange as the indicator. The mole fraction of neodymium oxide in the solid solution was computed from the relative amount of thorium and neodymium thus estimated. Their bulk and theoretical densities were determined by immersion and X-ray techniques.

### 2.2. X-ray diffraction studies

For characterization by X-ray powder diffraction, the sintered pellet was ground to obtain ~100 μm size particles. The XRD experiment was performed using Ni filtered Cu Kα radiation (λ = 1.54098 Å), in a Philips X′pert MPD system equipped with a graphite monochromator and a scintillation detector. The X-ray diffraction pattern was recorded in the two theta range, $20^\circ < 2\theta < 80^\circ$. Peak positions and the relative intensities were estimated using the peak-fit program of the Philips X′pert Plus software. The calibration of the diffractometer was carried out using silicon and α-alumina, standard reference materials. Good representative samples containing 23.8 and 42.5 mol% $NdO_{1.5}$ have been used for thermal expansion studies.

### 2.3. Thermal expansion studies

The thermal expansion characteristics of the solid solutions were studied from room temperature to 2000 K using HTXRD. The HTXRD studies were performed in a Philips-X'pert MPD® system, equipped with the Bühler® high vacuum heating stage. Typical instrument related parameters were operating voltage of 40 kV; current of 45 mA for the X-ray tube; scan speed of $0.02^\circ\ s^{-1}$ with a counting time of 6 s per step and an angular range ($2\theta$) of 20–80°. The heating stage consisted of a thin (~80 μm) resistance heated tantalum foil, on top of which the sample was placed. The temperature was measured by a W–Re thermocouple, which was spot-welded to the bottom of the tantalum heater. The temperature was controlled to an accuracy of about ±1 K. The diffraction studies were performed using Cu Kα radiation in the Bragg-Brentano geometry, at a temperature interval of 50 K up to 2000 K. A heating rate of 1 K $min^{-1}$ and a holding time of 60 min at each temperature of measurement were adopted. The specimen stage was flushed with high purity argon before the start of every experimental run and a vacuum level of about $10^{-5}$ mbar was maintained throughout the experiment. Acquisition and preliminary analysis of data were performed by the Philips X'pert Pro® software, although at a latter stage, we resorted to an independent processing of the raw data for a precise determination of the peak position.

### 2.4. X-ray photoelectron spectroscopy (XPS) studies

The X-ray photoelectron spectrometer used in this study is from VG ESCALAB MK200X Ltd., equipped with 150 mm hemispherical analyzer. The analyzer chamber is kept at $1.7 \times 10^{-10}$ mbar during measurements. A twin anode X-ray source is provided in the analyzer chamber for operation with Mg Kα (1253.6 eV) or Al Kα (1486.6 eV) radiations. An ion source is also provided for sputter-etch cleaning of specimens with inert gas ions of energies up to 10 KeV and beam currents of the order of ~10 μA. The electron energy analyzer was operated in the constant analyzer energy (CAE) mode, where the analyzer energy is fixed during a spectrum, that is the analyzer allowed only electrons with a particular energy to pass through. In this study, the spectra were collected using Al Kα X-ray source and with 20 eV pass energy of the analyzer. The data acquisition and processing were carried out using the Eclipse software. The instrument was calibrated with Au $4f_{7/2}$ line at 84.0 eV with 1.6 eV FWHM [19] for the specimen al Au film on Si substrate [20].

## 3. Results

### 3.1. Thermal expansion studies

In Table 1, the density versus composition data obtained in the present study are listed. As may be seen, for each composition the X-ray density is always higher than the corresponding

Table 1
Listing of composition, lattice parameter, bulk and theoretical densities of $Th_{1-x}Nd_xO_2$ system

| Solid solution no. | Mole fraction of $NdO_{1.5}$ | Lattice parameter (nm) | Bulk density ($10^{-3}$ kg m$^{-3}$) | X-ray density ($10^{-3}$ kg m$^{-3}$) | Percentage theoretical density |
|---|---|---|---|---|---|
| 1 | 6.1 | 0.5598 | 9.20 | 9.79 | 93.9 |
| 2 | 13.1 | 0.5604 | 8.91 | 9.53 | 93.5 |
| 3 | 18.7 | 0.5610 | 8.72 | 9.31 | 93.6 |
| 4 | 23.8 | 0.5615 | 8.58 | 9.12 | 94.0 |
| 5 | 28.7 | 0.5624 | 8.37 | 8.92 | 93.9 |
| 6 | 31.9 | 0.5626 | 8.24 | 8.80 | 93.7 |
| 7 | 35.1 | 0.5630 | 8.12 | 8.68 | 93.6 |
| 8 | 37.2 | 0.5633 | 8.05 | 8.60 | 93.6 |
| 9 | 42.5 | 0.5638 | 7.96 | 8.48 | 93.9 |
| 10 | 45.7 | 0.5640 | 7.89 | 8.39 | 94.1 |
| 11 | 46.2 | 0.5647 | 7.83 | 8.26 | 94.8 |
| 12 | 47.6 | 0.5650 | 7.79 | 8.23 | 94.7 |
| 13 | 49.7 | 0.5651 | 7.72 | 8.18 | 94.4 |
| 14 | 51.8 | 0.5652 | 7.69 | 8.11 | 94.9 |
| 15 | 54.6 | 0.5651 | 7.64 | 8.04 | 95.0 |
| 16 | 58.3 | 0.5652 | 7.60 | 7.95 | 95.6 |
| $ThO_2$ | Pure | 0.5597 | 9.70 | 10.00 | – |
| $Nd_2O_3$ | Pure | $a = 0.38297$, $c = 0.59987$ | 7.28 | 7.33 | – |

The lattice parameter values of pure $ThO_2$ and $Nd_2O_3$ taken from ICDD data, are also listed for reference.

bulk density, attesting to the presence of porosity in the sintered samples. However, it is gratifying to note that even without the addition of any binder and besides adopting relatively a low-sintering temperature (1473 K), we could achieve about 94% of theoretical density. This advantage derives from the enhanced homogeneity of the initial powder mix obtained through the co-precipitation route [21].

From Fig. 1, it is evident that with increasing concentration of $NdO_{1.5}$ in the solid solution, the various peak positions evince a mild shift towards the lower angle side. This is consistent with the overall increase in lattice parameter of the solid solution that follows upon the addition of neodymium oxide to thoria. Further, this point is also corroborated by our bulk density data in that there is a gradual decrease in density with increasing mole fraction of $NdO_{1.5}$ (see Table 1). In Fig. 2, the composition dependence of lattice parameter of the solid solution is graphically displayed. It emerges from Fig. 2 that the steady increase in lattice parameter of the thoria matrix with respect to the addition of neodymium oxide reaches a maximum, at about 45–46 mol%; after which an almost constant behaviour is noticed. The onset of this solubility limit is also clearly reflected in the corresponding XRD profiles (Fig. 1). It is instructive to note from Fig. 1, that up to about 45.7 mol% $NdO_{1.5}$ in $ThO_2$, the XRD profiles are qualitatively similar. But upon reaching the solubility limit say, about 45.7 mol%, small, yet distinctly visible humps are noticed in the XRD profile. These are marked by small arrows in Fig. 1. With further additions of $NdO_{1.5}$, these humps begin to manifest as distinct peaks that are characteristic of $Nd_2O_3$ structure. However, the full pattern that is characteristic of pure $NdO_{1.5}$ has not been obtained even up to additions of about 58.3 mol% $NdO_{1.5}$ (note the pattern for 58.3 mol% solid solution in Fig. 1). This suggests that for $NdO_{1.5}$ concentrations higher than about 46.2 mol%, we have already reached the limit of solubility and in fact made an entry into the two-phase field. Combining this information with the lattice parameter variation given in Fig. 2, we estimate that within the resolution limit set by our experimental techniques, the maximum solubility of $NdO_{1.5}$ in $ThO_2$

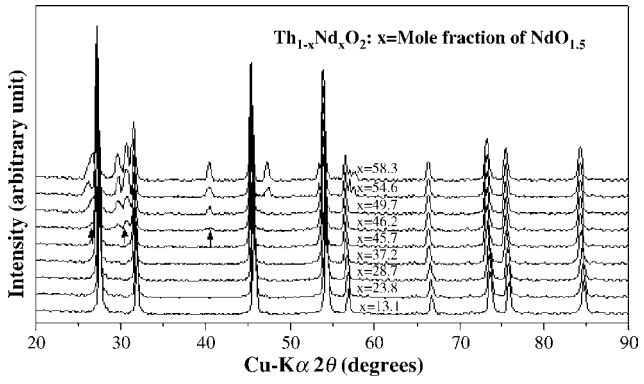


Fig. 1. The X-ray diffraction profiles (Cu Kα radiation) obtained for various concentrations of $NdO_{1.5}$ in $ThO_2$ are presented as a collage. Note that for neodymium oxide concentrations exceeding 45.7 mol%, small humps have started appearing in the XRD profile. These humps are marked by arrows in the figure.

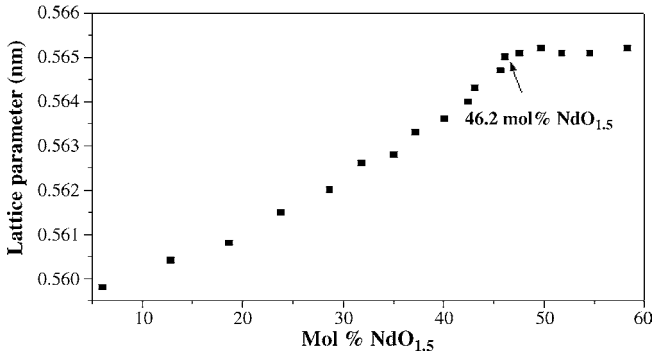


Fig. 2. Composition dependence of lattice parameter in $Th_{1-x}Nd_xO_2$ system is graphically illustrated. The plateau in the curve occurring at a $NdO_{1.5}$ mol% 45.7–46.2 represents the upper limit of solubility in this system.

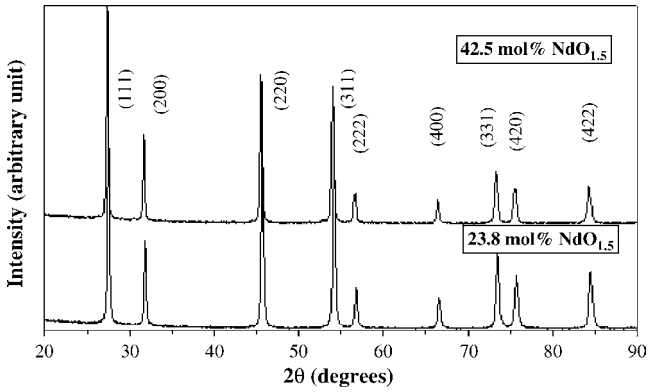


Fig. 3. Room temperature XRD pattern of the $ThO_2$—$NdO_{1.5}$ solid solutions.

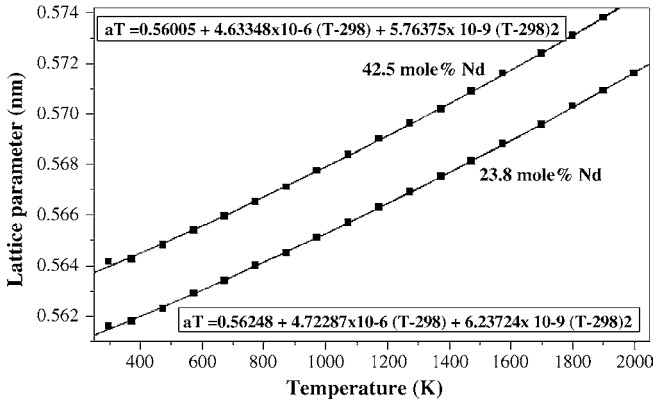


Fig. 4. The temperature variation of corrected lattice parameter of $ThO_2$—$NdO_{1.5}$ solid solutions is illustrated.

from room temperature to a temperature of about 1473 K is in the range 45.7–46.2 mol%.

In Fig. 3, we present the room temperature (298 K) XRD patterns of two representative solid solutions of $ThO_2$ with 23.8 and 42.5 mol% of $NdO_{1.5}$. The lattice parameter ($a$) in each case was estimated by considering the eight major reflections of the $CaF_2$ structure (see Fig. 3). Finally an effective high angle corrected lattice parameter at each temperature is obtained by the standard Nelson-Riley extrapolation procedure [22]. Fig. 4 shows the effective lattice parameter thus obtained as a function of temperature for both compositions. The lattice parameter data as a function of temperature is also listed in Table 2.

For the purpose of calculating thermal expansivity, the corrected lattice parameter data with temperature ($K$) are fitted to a second-degree polynomial in the temperature increment ($T - 298$). The relevant fit expression is given below for $ThO_2$—23.8 mol% neodymium oxide solid solution:

$$a\,(\mathrm{nm}) = 0.56248 + 4.72287 \times 10^{-6}(T - 298) + 6.23724 \times 10^{-9}(T - 298)^2. \quad (1)$$

A similar fit for $ThO_2$ – 42.5 mol% neodymium oxide solid solution is yielded by the following expression:

$$a\,(\mathrm{nm}) = 0.56005 + 4.63348 \times 10^{-6}(T - 298) + 5.76375 \times 10^{-9}(T - 298)^2 \quad (2)$$

where, $T$ is in Kelvin. Once the lattice parameter is known as a function of temperature, it is possible to estimate the instantaneous ($\alpha_L$-instantaneous), mean ($\alpha_L$-mean) and relative ($\alpha_L$-relative) linear thermal expansion coefficients by the following

Table 2
The lattice parameter as a function of temperature, instantaneous ($\alpha_i$ instantaneous) mean ($\alpha_m$) and linear thermal expansion (%)

| HT-XRD data on $ThO_2$—$NdO_{1.5}$ solid solution | | | | | | | | |
|---|---|---|---|---|---|---|---|---|
| 23.8 mol% $NdO_{1.5}$ | | | | | 42.5 mol% $NdO_{1.5}$ | | | |
| $T$ (K) | $a$ (nm) | $\alpha_i$ ($10^{-6}$ K$^{-1}$) | $\alpha_m$ ($10^{-6}$ K$^{-1}$) | Expansion (%) ($10^{-6}$ K$^{-1}$) | $a$ (nm) | $\alpha_i$ ($10^{-6}$ K$^{-1}$) | $\alpha_m$ ($10^{-6}$ K$^{-1}$) | Expansion (%) ($10^{-6}$ K$^{-1}$) |
| 298 | 0.5615 | 8.97 | 8.97 | 00 | 0.5640 | 9.14 | 9.14 | 00 |
| 373 | 0.5618 | 9.11 | 9.12 | 0.06 | 0.5644 | 9.30 | 9.31 | 0.0622 |
| 473 | 0.5624 | 9.30 | 9.31 | 0.15 | 0.5649 | 9.51 | 9.53 | 0.1564 |
| 573 | 0.5629 | 9.48 | 9.51 | 0.25 | 0.5654 | 9.73 | 9.75 | 0.2527 |
| 673 | 0.5634 | 9.67 | 9.70 | 0.34 | 0.5660 | 9.94 | 9.97 | 0.3513 |
| 773 | 0.5640 | 9.85 | 9.90 | 0.44 | 0.5665 | 10.15 | 10.19 | 0.4521 |
| 873 | 0.5645 | 10.03 | 10.09 | 0.54 | 0.5671 | 10.36 | 10.41 | 0.5551 |
| 973 | 0.5651 | 10.22 | 10.28 | 0.64 | 0.5677 | 10.57 | 10.63 | 0.6603 |
| 1073 | 0.5657 | 10.40 | 10.48 | 0.75 | 0.5683 | 10.78 | 10.85 | 0.7678 |
| 1173 | 0.5663 | 10.58 | 10.67 | 0.85 | 0.5689 | 10.99 | 11.07 | 0.8774 |
| 1273 | 0.5669 | 10.76 | 10.87 | 0.96 | 0.5696 | 11.20 | 11.30 | 0.9893 |
| 1373 | 0.5675 | 10.94 | 11.06 | 1.07 | 0.5702 | 11.41 | 11.52 | 1.1033 |
| 1473 | 0.5681 | 11.12 | 11.25 | 1.18 | 0.5709 | 11.62 | 11.74 | 1.2196 |
| 1573 | 0.5688 | 11.30 | 11.45 | 1.30 | 0.5715 | 11.83 | 11.96 | 1.3381 |
| 1700 | 0.5696 | 11.53 | 11.70 | 1.44 | 0.5724 | 12.09 | 12.24 | 1.4918 |
| 1800 | 0.5703 | 11.71 | 11.89 | 1.56 | 0.5731 | 12.30 | 12.46 | 1.6153 |
| 1900 | 0.5709 | 11.88 | 12.08 | 1.68 | 0.5738 | 12.51 | 12.68 | 1.7410 |
| 2000 | 0.5716 | 12.06 | 12.28 | 1.80 | 0.5745 | 12.72 | 12.90 | 1.8689 |

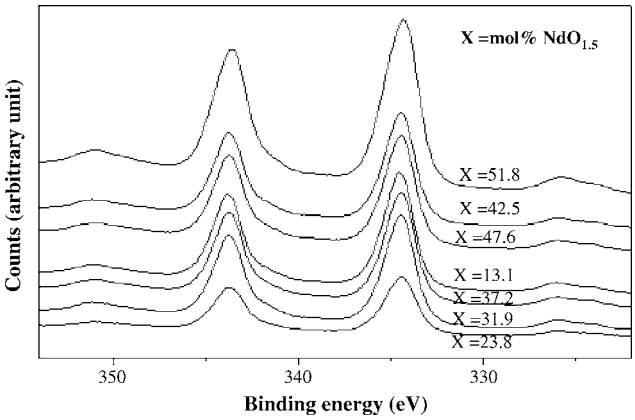


Fig. 5. Th 4f photoelectron spectra for $ThO_2$—$NdO_{1.5}$ solid solutions.

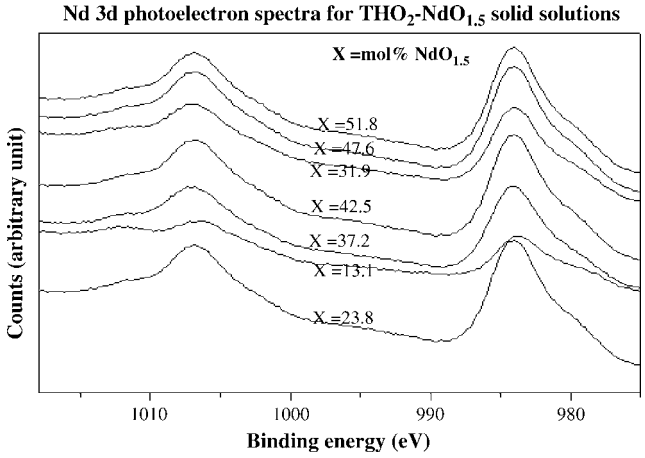


Fig. 6. Nd 3d photoelectron spectra for $ThO_2$—$NdO_{1.5}$ solid solutions.

relations:

$$\alpha_L \text{instantaneous} = (1/a_T)(da_T/dT). \quad (3)$$

$$\alpha_L \text{mean} = (1/a_{298}) \times \{(a_T - a_{298})/(T - 298)\}. \quad (4)$$

$$\alpha_L \text{relative} = (1/a_{298})(da_T/dT). \quad (5)$$

$$\text{Expansion}\,(\%) = 100 \times \{(a_T - a_{298})/a_{298}\}. \quad (6)$$

In the above expression, $a_T$ represents the lattice parameter at temperature $T$ and $a_{298}$ the corresponding value at 298 K. The percentage linear thermal expansion of the solid solutions were computed using Eq. (6).

### 3.2. Binding energies

$Th4f_{7/2}$ and $Nd3d_{5/2}$ photoelectron spectra for $ThO_2$—$NdO_{1.5}$ solid solutions containing 13.1, 23.8, 31.9, 37.2, 42.5, 47.6 and 51.8 mol% $NdO_{1.5}$ were recorded to understand the valence state of thorium and neodymium in the mixed oxides and the change in its electronic structure due to the formation of the solid solution. Figs. 5 and 6 shows the Th $4f_{7/2}$, Nd $3d_{5/2}$ photoelectron spectra for $ThO_2$—$NdO_{1.5}$ solid solutions, respectively. The peak positions and peak widths of Th $4f_{7/2}$ and Nd $3d_{5/2}$ photoelectron spectra are listed in Table 3. From the data in this table, it is clear that these parameters have not changed significantly from corresponding values for pure thorium and neodymium [23–25]. The peak positions indicate that thorium and neodymium are in +4 and +3 states, respectively.

## 4. Discussion

In Fig. 7, we present the percentage linear thermal expansion obtained for these solid solutions. For the sake of comparison, we also present in Fig. 7, the mean thermal expansivity value

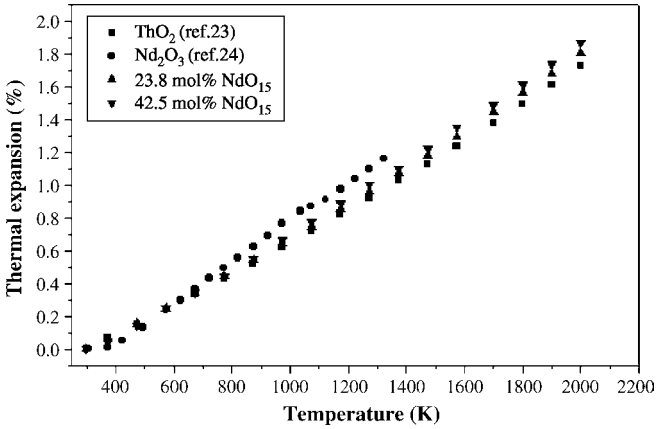


Fig. 7. The percentage linear thermal expansion estimated from the lattice parameter of $ThO_2$—$NdO_{1.5}$ solid solutions are plotted together with the corresponding data on pure $ThO_2$ and neodymium oxide.

Table 3
Binding energy of specified atomic levels for Th and Nd in $ThO_2$—$NdO_{1.5}$ solid solutions

| Sl. no. | Mol% of $NdO_{1.5}$ | Binding energies | | FWHM | | References |
|---|---|---|---|---|---|---|
| | | Th $4f_{7/2}$ | Nd $3d_{5/2}$ | Th $4f_{7/2}$ | Nd $3d_{5/2}$ | |
| 1 | 00 | 333.8 | – | 1.8 | – | [23,24] |
| 2 | 13.1 | 334.2 | 984.5 | 2.0 | 2.1 | This study |
| 3 | 23.8 | 334.1 | 984.4 | 1.9 | 2.0 | This study |
| 4 | 31.9 | 334.2 | 984.3 | 1.8 | 2.1 | This study |
| 5 | 37.2 | 334.1 | 984.6 | 2.0 | 2.2 | This study |
| 6 | 42.5 | 333.9 | 984.5 | 2.1 | 2.0 | This study |
| 7 | 47.6 | 334.1 | 984.6 | 1.9 | 2.1 | This study |
| 8 | 51.8 | 334.2 | 984.5 | 2.0 | 2.0 | This study |
| 9 | 100 | – | 984.5 | – | 2.1 | [25] |

Table 4
Temperature range, composition and thermal expansion data reported by Mathews et al. and the present study for comparison

| Sl. no | Mol% $NdO_{1.5}$ | $\alpha_l$ (293–1123 K) dilatometry $10^{-6}$ ($K^{-1}$) | $\alpha_a$ (293–1123 K) HTXRD $10^{-6}$ ($K^{-1}$) | $\alpha_a$ (293–1473 K) HTXRD $10^{-6}$ ($K^{-1}$) | References |
|---|---|---|---|---|---|
| 1 | 10 | 9.48 | 9.70 | 10.60 | [13,14] |
| 2 | 20 | 9.69 | 9.90 | 10.76 | [13,14] |
| 3 | 23.8 | – | 10.67 (1173 K) | 11.25 | This study |
| 4 | 30 | 9.91 | 10.55 | 10.91 | [13,14] |
| 5 | 40 | 10.34 | 10.76 | 11.06 | [13,14] |
| 6 | 42.5 | – | 11.07 (1173 K) | 11.74 | This study |
| 7 | 50 | 10.77 | 10.99 | 11.06 | [13,14] |

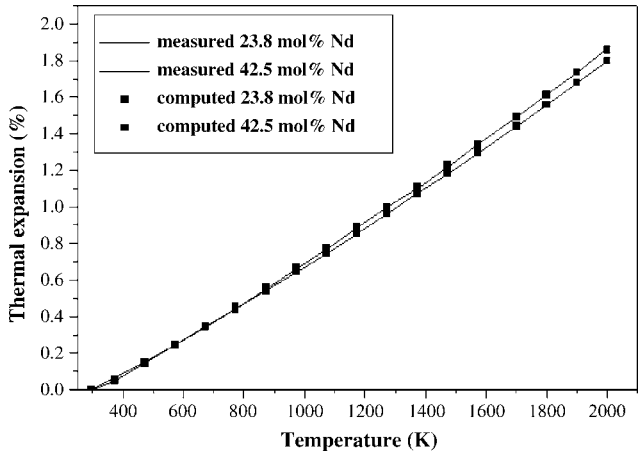


Fig. 8. Measured and computed (mol% weighted average) thermal expansion are compared for $ThO_2$–$NdO_{1.5}$ solid solutions containing 23.8 and 42.5 mol% $NdO_{1.5}$.

for pure thoria [26] and neodymium oxide [27] taken from the literature.

It must be mentioned that to the best of our knowledge, only few HTXRD based lattice thermal expansion and bulk thermal expansion data for $ThO_2$–$NdO_{1.5}$ solid solutions are available in the open literature. The room temperature lattice parameter values estimated in the present study for the $ThO_2$–$NdO_{1.5}$ solid solutions containing 23.8 and 42.5 mol% $NdO_{1.5}$ were found to be 0.5615 and 0.5640 nm. From Fig. 4, it is observed that the lattice parameter of both the solid solutions increases progressively with increasing temperature. They are nearly independent of composition up to about 700 K. This suggests that the thermal expansion of the solid solutions and pure thoria are almost equal up to 700 K. Above 700 K, the values of linear thermal expansion of thoria–neodymium oxide solid solutions are found to lie in between those of pure thoria and neodymium oxide end members. Fig. 8 compare the percentage linear thermal expansion measured in this study with that based on weighted average of the individual $ThO_2$ and neodymium oxide. It is evident from these figures that the measured thermal expansion coefficients show a good agreement with the estimated values based on the law of weighted mole fractions. It is also interesting to note that the agreement is observed up to 2000 K, the highest temperature recorded in this study. Hence, it is inferred that the behaviour of stoichiometric $ThO_2$–$NdO_{1.5}$ solid solutions containing 23.8 and 42.5 mol% $NdO_{1.5}$ are almost ideal, at least up to 2000 K.

Thermal expansion characteristic of $ThO_2$–$NdO_{1.5}$ solid solution containing 10, 20, 30, 40 and 50 mol% neodymium oxide were studies by Mathews et al. [13,14] in the temperature range from room temperature to 1123 K using dilatometer and up to 1473 K using HTXRD. In this study the lattice thermal expansion measurement carried out from room temperature to 2000 K using HTXRD. The coefficient of average linear bulk and lattice thermal expansion given in the Ref. [13,14] along with the data obtained in the present study are presented in the Table 4 for comparison. It is seen from the Table 4 the average bulk and lattice thermal expansion coefficient of solid solution reported by them is comparable that the values reported in this study up to 1473 K. Beyond 1473 K, no values are available in the report other than the values reported in the present study.

## 5. Conclusion

A series of solid solution of $ThO_2$–$NdO_{1.5}$ were synthesised and thermal expansion studies were carried out for two good representative compositions in the temperature range from room temperature to 2000 K using high temperature X-ray diffraction. The percentage linear thermal expansion in this temperature range, for $ThO_2$–$NdO_{1.5}$ solid solutions containing 23.8 and 42.5 mol% $NdO_{1.5}$ are 1.80 and 1.87, respectively. It is suggested that the solid solutions are stable up to 2000 K. It is also suggested that the effect and nature of the dopant are the important parameters influenced in the thermal expansion of the $ThO_2$. The XPS study of the solid solutions indicates that thorium and neodymium are in +4 and +3 oxidation state, respectively, in all the solid solutions.

## Acknowledgements

The authors are grateful to Dr. P.R. Vasudeva Rao and Dr. T.G.Srinivasan for their sustained encouragement and support during the course of work. The authors also express their sincere gratitude to Dr. Santanu Bera for recording the XPS patterns of various samples.

## References

[1] R. Chidambaram, M. Srinivasan, I. Kimura (Eds.), Proceedings of the Indo-Japan Seminar on Thorium Utilization, Bombay, Indian Nuclear society and Atomic Energy Society of Japan, December, 1990.
[2] H. Kleykamp, J. Nucl. Mater. 131 (1985) 221.

[3] E.H.P. Cordfunke, R.J.M. Konings, J. Nucl. Mater. 152 (1988) 301.
[4] C.E. Johnson, I. Johnson, P.E. Blackburn, C.E. Crouthamel, Reactor Technol. 15 (1972–1973) 303.
[5] K. Une, M. Oguma, J. Nucl. Sci. Technol. 20 (1983) 844.
[6] A.M. Diness, B. Rustam, J. Mater. Sci. 4 (1969) 613.
[7] P.S. Murti, C.K. Mathews, High Temp. High Press. 22 (1990) 379.
[8] C.A. Alexander, et al., Fission Product Transport in Reactor Accidents, Hemisphere, New York, 1990, p. 127.
[9] C. Keller, U. Berndt, H. Engerer, L. Leitner, J. Solid State Chem. 4 (1972) 453.
[10] F. Sibieude, M. Foex, J. Nucl. Mater. 56 (1975) 229.
[11] G. Panneerselvam, M.P. Antony, T. Vasudevan, Mater. Lett. 58 (2004) 3192.
[12] P. Srirama Murti, C.K. Mathews, J. Phys. D: Appl. Phys. 24 (1991) 2202.
[13] M.D. Mathews, B.R. Ambekar, A.K. Tyagi, J Alloys Compd. 386 (2005) 234.
[14] M.D. Mathews, B.R. Ambekar, A.K. Tyagi, J. Nucl. Mater. 341 (1) (2005) 19.
[15] G. Panneerselvam, M.P. Antony, P.R. Vasudeva Rao, in: Proceedings of the International Conference on Ceramic Processing, ICCP-04, Mumbai, December 21–24, 2004, p. 34.
[16] M. Ugajin, T. Shiratoru, K. Shiba, J. Nucl. Mater. 84 (1979) 26.
[17] R. Pribil, V. Vesely, Talanta 10 (1963) 899.
[18] I.M. Yurist, P.M. Zaitsev, Zhurnal Analiticheskoi Khimi. 38 (1983) 1706.
[19] D.K. Sarkar, S. Bera, S. Dhara, K.G.M. Nair, S.V. Narasimhan, S. Chowdhury, Appl. Surf. Sci. 120 (1997) 159.
[20] C.J. Powell, Surf. Interface Anal. 23 (1995) 121.
[21] G.D. White, L.A. Bray, P.E. Hart, J. Nucl. Mater. 96 (1981) 305.
[22] B.D. Cullity, Element of X-ray Diffraction, 2nd ed., Eddision Weseley Publishing Co, Reading, MA, 1978.
[23] C.D. Wabner, W.M. Riggs, L.E. Davis, J.F. Moulde, G.E. Muilenberg (Eds.), Handbook of XPS (USA), 1979.
[24] B.W. Veal, D.J. Lam, H. Diamond, H.R. Hoekstra, Phys. Rev. B.15 (6) (1977) 2929.
[25] B.W. Veal, D.J. Lam, Phys. Rev. B.10 (12) (1974) 4902.
[26] J. Belle, R.M. Berman, Thorium dioxide: Properties and Nuclear Applications DOE/NE-0060, 1984.
[27] E. Mistler, G.L. Ploetz, J.A. Smith, J. Am. Cram Soc. 56 (1963) 561.